A review on recent results on on/off reconstruction of optical states

G. Brida[1], **M. Genovese**[1], **M. Gramegna**[1], **A. Meda**[1], **S. Olivares**[2,3], **M. G. A. Paris**[3,2,4], **F. Piacentini**[1], **E. Predazzi**[3], **P. Traina**[1]

[1] *I.N.RI.M., Strada delle Cacce 91, Torino, Italia*

[2] *CNISM UdR Milano Università, I-20133 Milano, Italia*

[3] *Dipartimento di Fisica dell'Università di Milano, I-20133 Milano, Italia*

[4] *Institute for Scientific Interchange, I-10133 Torino, Italia and*

[5] *INFN and Dipartimento di Fisica Teorica dell'Università di Torino, via P. Giuria 1, 10125 Torino, Italia*

The knowledge of the density matrix of a quantum state plays a fundamental role in several applications, from quantum information to Standard Quantum Mechanics foundations investigation.
Recently, a method has been implemented in order to obtain the reconstruction of the (diagonal) elements of the density matrix exploiting the information achievable with realistic on/off detectors (e.g. silicon avalanche photo-diodes). Purpose of this paper is to introduce this on/off method and present the last experimental results obtained with it in several different cases.

OCIS codes: 42-50-p, 03.67.Hk, 42.62.Eh

1. Introduction

The knowledge of density matrix of a quantum state is fundamental for several applications, ranging from quantum information[1] to the foundations of quantum mechanics[2] and quantum optics[3,4,5,6,7,8,9,10,11]. Many efforts have been made to find reliable methods to fully or partially reconstruct the density matrix especially in the photon number basis. In this last case, the reconstruction of the diagonal elements, i.e., the photon statistics, is of extreme relevance for a first characterization of the state. Nevertheless, the choice of a detector with internal gain suitable for the measurement is not trivial when the flux of the photons to be counted is such that more than one photon is detected in the time-window of the measurement, which is set by the detector pulse-response, or by an electronic gate on the detector output, or by the duration of the light pulse. In this case, we need a congruous linearity in the internal current amplification process: each of the single electrons produced by the different photons in the primary step of the detection process (either ionization or promotion to a conduction band) must experience the same average gain and this gain must have sufficiently low spread. The fulfillment of both requisites is necessary for the charge integral of the output current pulse be proportional to the number of detected photons. Photon detectors that can operate as photon counters are rather rare. Among these, Photo-Multiplier Tubes (PMT's)[13] and hybrid photodetectors[14] have the drawback of a low quantum efficiency, since the detection starts with the emission of an electron from the photocathode. Solid state detectors with internal gain, in which the nature of the primary detection process ensures higher efficiency, are still under development. Highly efficient thermal photon counters have also been used, though their operating conditions are still extreme (cryogenic conditions) to allow common use[15,16]. The advent of quantum tomography provided an alternative method to measure photon number distributions[17]. However, the tomography of a state, which has been applied to several quantum states[10], needs the implementation of homodyne detection, which in turn requires the appropriate mode matching of the signal with a suitable local oscillator at a beam splitter. Such mode matching is a particularly challenging task in the case of pulsed optical fields.

Photodetectors that are usually employed in quantum optics such as Avalanche Photo-Diodes (APD's) operating in the Geiger mode[16,18] seem to be by definition useless as photon counters. They are the solid state photodetectors with the highest quantum efficiency and the greatest stability of the internal gain. However, they have the obvious drawback that the breakdown current is independent of the number of detected photons, which in turn cannot be determined. The outcome of these APD's is either "off" (no photons detected) or "on" *i.e.* a "click", indicating the detection of one or more photons. Actually, such an outcome can be provided by any photodetector (PMT, hybrid photodetector, cryogenic thermal detector) for which the charge contained in dark pulses is definitely below that of the output current pulses corresponding to the detection of at least one photon. Note that for most high-gain PMT's the anodic pulses corresponding to no photons detected can be easily discriminated by a threshold from those corresponding to the detection of one or more photons.

It may thus appear surprising at first that, among the various theoretical studies[19,20,21,22] that have been addressed to achieve the reconstruction of the (diagonal) elements of the density matrix exploiting the information achievable with realistic detectors, a favourable experimental test has been found in[23,24,25,26,27], where a high-

fidelity reconstruction of the statistics of mono-partite and bi-partite quantum optical states was obtained by using on/off detectors[21,22].

Purpose of this paper is to introduce this on/off method and present the last experimental results obtained with it.

2. Reconstruction method: diagonal elements of monopartite systems

Let us consider a single-mode quantum optical state. All the accessible information on the state is expressed in its *density matrix* $\hat{\rho}$, which in the photon number basis reads:

$$\hat{\rho} = \sum_{n,m=0}^{\infty} \rho_{nm} |n\rangle\langle m| \tag{1}$$

In particular, the information regarding photon distribution of the state is given by the diagonal elements $\rho_n \equiv \rho_{nn}$ of this matrix.

In this section we are going to show how reconstruction of the ρ_n's for a general quantum optical state is possible via on/off detectors.

Assuming that our state is to be revealed by a two-level detector, like silicon APDs (avalanche photo-diodes) or a photomultiplier operating in Geiger mode, i.e. a detector discriminating only between vacuum, "0", and light passage, "1", with quantum efficiency $0 \leq \eta \leq 1$, the measurement process is described by a two-value *positive operator-valued measure* (POVM):

$$\Pi_0(\eta) = \sum_{n=0}^{\infty} (1-\eta)^n |n\rangle\langle n|, \quad \Pi_1(\eta) = \mathrm{I} - \Pi_0(\eta). \tag{2}$$

The non-detection probability, $p_0 = \mathrm{Tr}\left[\rho \Pi_0(\eta)\right]$, is thus given by:

$$p_0(\eta) = \sum_{n=0}^{\infty} (1-\eta)^n \rho_n = \sum_{n=0}^{\infty} A_n(\eta)\rho_n, \tag{3}$$

and the detection probability is $p_1(\eta) = 1 - p_0(\eta)$. Supposing to have the possibility of varying the quantum efficiency η of our detector, we can perform K measurements on our optical state, each one with a different η, building the ensemble:

$$\mathbf{P_0} \equiv \left\{ p_\mu : \quad p_\mu = \sum_{n=0}^{\infty} A_{\mu n}\rho_n \qquad \mu = 1, ..., K \right\} \tag{4}$$

where we define $A_{\mu n} \equiv A_n(\eta_\mu)$.

If we restrict ourselves to the approximation $\rho_n \simeq 0 \ \forall n > N$ and we are able to perform at least K different measurements ($K \geq N+1$), for the non-click probability ensemble (4) we can write the linear system:

$$\mathbf{P_0} = \mathbb{V} \cdot \rho \qquad (\rho \equiv \{\rho_i, \quad i = 0, ..., N\}) \tag{5}$$

where the coefficients matrix $\mathbb{V}$ ($\forall \eta_\mu : \ i \neq j \Rightarrow \eta_i \neq \eta_j$) is a nonsingular Vandermonde matrix of order $N+1$. Since the ρ array reconstruction via matrix inversion would require a huge and almost impossible to obtain number of experimental runs to avoid very large numerical fluctuations, the need of a faster solution protocol leads to consider eq.s (3) and (4) as a statistical model for the ρ_n coefficients, presenting a *linear positive* problem to be solved by means of the *maximum likelihood* (ML) method[28]. By using the *expectation maximization* (EM) algorithm, after imposing the normalization constraint $\sum_n \rho_n = 1$, we arrive at the iterative formula:

$$\rho_n^{(i+1)} = \rho_n^{(i)} \sum_{\mu=1}^{K} \left[\frac{A_{n\mu}}{\sum_{\lambda=1}^{K} A_{n\lambda}} \cdot \frac{f_\mu}{p_\mu\left[\left\{\rho_n^{(i)}\right\}\right]} \right] \tag{6}$$

with:

$$\begin{aligned} &\rho_n^{(i)} = \text{ reconstructed } \rho_n \text{ at the } i\text{-th iteration;} \\ &f_\mu = \tfrac{n_{0\mu}}{n_\mu} = \text{ non-click events fraction;} \\ &p_\mu\left[\left\{\rho_n^{(i)}\right\}\right] = \text{ evaluated non-click probability} \\ &\qquad\qquad \text{with the reconstructed } \rho_n^{(i)} \end{aligned} \tag{7}$$

where $n_{0\mu}$ and n_μ are respectively the registered non-click events and the total experimental runs performed with quantum efficiency η_μ[20,21].

The confidence interval on the determination of the element $\rho_n^{(i)}$ can be estimated in terms of the variance:

$$\sigma_n^2 = (KF_n)^{-1} \tag{8}$$

being F_n the Fisher information on the reconstructed element, given by the formula:

$$F_n = \sum_{\mu=1}^{K} \frac{1}{l_\mu} \left(\left.\frac{\partial l_\mu}{\partial \rho_n}\right|_{\rho_n = \rho_n^{(i)}} \right)^2 \tag{9}$$

where:

$$l_\mu = \frac{\sum_{n=0}^{N} A_{\mu n}\rho_n}{\sum_{\mu=1}^{K}\left(\sum_{n=0}^{N} A_{\mu n}\rho_n\right)}.$$

To check the convergence of this algorithm, we look at the error parameter $\epsilon^{(i)}$, defined as:

$$\epsilon^{(i)} = K^{-1} \sum_{\mu=1}^{K} \left| f_\mu - p_\mu\left(\left\{\rho_n^{(i)}\right\}\right) \right|, \tag{10}$$

stopping the iteration number when the value of $\epsilon^{(i)}$ goes below a certain threshold.

Finally, the fidelity of our reconstructed photon statistics with respect to the theoretical one, $\rho_n^{(theo)}$, is given by the formula:

$$G^{(i)} = \sum_{n=0}^{N} \sqrt{\rho_n^{(theo)} \cdot \rho_n^{(i)}}. \tag{11}$$

Several tests on this protocol have been made, all of them successfully achieving a good agreement between the reconstructed ρ_n and the expected ones. As a first example, we consider a weak coherent state generated by a cw He-Ne laser emission. In fig.1 is possible to view the corresponding reconstructed photon number distribution (compared to the theoretical one). A best fit procedure shows that the reconstructed photon number distribution is compatible with the one expected for a coherent state with a mean number of photons $\langle n\rangle = 5.39$

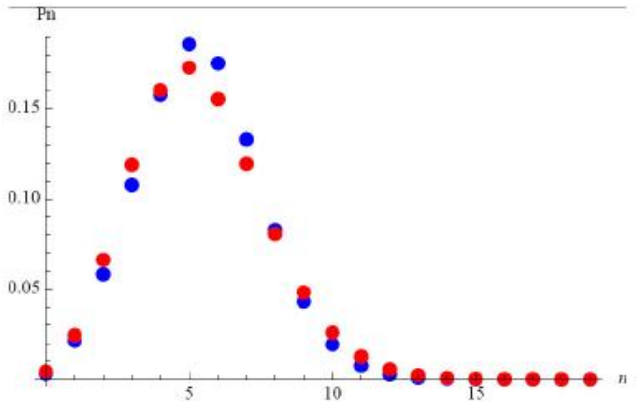

Fig. 1. *Reconstruction of the photon distribution for the weak coherent state (blue dots) compared to simulated Poissonian distribution (red dots). The data are compatible with the predictions for a coherent state with a mean number of photons* $\langle n\rangle = 5.39$

As a second example, we mention the experiment on single-photon states generated by producing PDC heralded photons[23,24]where, a pair of correlated photons (of different polarization) was generated by pumping a type-II β-barium-borate (BBO) crystal with a CW argon ion laser beam (351 nm) in collinear geometry. After having split the photons of the pair by means of a polarizing beam splitter, the detection of one of the two by a silicon avalanche photodiode detector (SPCM-AQR-15, Perkin Elmer) was used to herald the presence of the second photon in the other channel (namely, a window of 4.9 ns was opened for detection in arm 2 in correspondence to the detection of a photon in arm 1); this "heralded" photon was then measured by another APD (SPCM-AQR-15, Perkin Elmer) preceded by an iris and an interference filter (IF) centered at 702 nm (4 nm of FWHM) inserted with the purpose of reducing the noise due to the stray light. The quantum efficiency of the detection apparatus was $\eta_{max} = 20\%$: lower quantum efficiencies were simulated by inserting calibrated neutral filters (NF) on the optical path.

The reconstructed statistics perfectly agreed with the expected ones: together with a dominant single photon component, a vacuum and double pair components were measured, respectively of $(2,7\pm0,2)\%$ and $((1,9\pm0,2)\%$ (in agreement with the theoretical values). Finally, we would like to acknowledge a recent measurement where the method was applied to stimulated PDC[29]. In this case we used a new algorithm where a constraint (on photon number) was introduced (through Lagrange multipliers), showing as this allows a very good reconstruction in critical cases.

3. Extension to the bipartite case: the theory

Since for many applications multipartite states are needed, our aim here is to extend our model of the previous section to this case as well. In particular, for the bipartite case (easily generalizable to the multipartite one), we will consider two propagation modes of our optical field (i.e. the two outputs of a beam splitter) and study both of them at the same time, trying to extend the previous formulas to this new framework[26].
To begin with, instead of the probabilities (3) we will have the *joint* click/no-click probabilities:

$$\begin{cases} p_{00}(\eta) = \sum_{n,k} A_n(\eta) A_k(\eta) \varrho_{nk} \\ p_{01}(\eta) = \sum_{n,k} A_n(\eta)[1 - A_k(\eta)] \varrho_{nk} \\ p_{10}(\eta) = \sum_{n,k} [1 - A_n(\eta)] A_k(\eta) \varrho_{nk} \\ p_{11}(\eta) = 1 - p_{00}(\eta) - p_{10}(\eta) - p_{01}(\eta) \end{cases} \tag{12}$$

where:

$$\varrho_{nk} = \langle nk|\varrho|nk\rangle \qquad \Big(|nk\rangle = |n\rangle \otimes |k\rangle\Big) \tag{13}$$

is the *joint photon distribution* of the state and η the quantum efficiency of the hypothetical detectors considered.

The above equations provide a relation between the statistics of the clicks of our detectors and the actual statistics of photons. Again, let us restrict our considerations to the case $\varrho_{nk} \simeq 0 \ \forall\, n,k \geq N$ (i.e. we "confine" our bipartite state into a $(N+1)\times(N+1)$ Hilbert space): if we can properly change the quantum efficiency of our system in such a way that K different measurements can be performed (with K different values η_μ, $\mu = 1,...,K$, ranging from $\eta_1 = \eta_{\min}$ to a maximum value $\eta_K = \eta_{\max}$), the whole amount of on/off detection statistics collected can give enough information to reconstruct the joint photon distribution of the bipartite state.

In details, by defining the vectors:

$$\mathbf{g} = \Big(p_{00}^{\eta_1},...,p_{00}^{\eta_K},p_{01}^{\eta_1},...,p_{01}^{\eta_K},p_{10}^{\eta_1},...,p_{10}^{\eta_K}\Big) \tag{14}$$

$$\mathbf{q} = (\varrho_{00},\varrho_{01},\varrho_{10},...) \tag{15}$$

$$\varrho_{nk} \to q_p \qquad \big(p = 1 + k + n(1+N)\big), \tag{16}$$

we can summarize the on/off statistics with the compact formula:

$$\mathbf{g} = \mathbb{B}\cdot\mathbf{q} \ \ \rightarrow \ \ g_\mu = \sum_{p=1}^{(N+1)^2} B_{\mu p} q_p \qquad \mu = 0,...,3K \tag{17}$$

where we have introduced the matrix $\mathbb{B}$ with entries:

$$[\mathbb{B}]_{\mu p} = \begin{cases} A_{\mu n} A_{\mu k} & \text{if} \quad \mu = 1, .., K \\ A_{\mu n}(1 - A_{\mu k}) & \text{if} \quad \mu = K+1, .., 2K \\ (1 - A_{\mu n}) A_{\mu k} & \text{if} \quad \mu = 2K+1, .., 3K \end{cases} \tag{18}$$

where $k = (p-1) \mathrm{mod}(1+N)$ and $n = (p-1-k)/(1+N)$.

In our conditions, eq. (17) represents a finite statistical linear model for the positive unknown q_p. Like in the monopartite case, by means of the maximum-likelihood (ML) principle we achieve a well approximated solution of this LINPOS problem with the iterative algorithm[28]:

$$q_p^{(i+1)} = q_p^{(i)} \left(\sum_{\mu=1}^{3K} B_{\mu p} \right)^{-1} \sum_{\mu=1}^{3K} \left[\frac{B_{\mu p} h_\mu}{g_\mu \left[\left\{ q_p^{(i)} \right\} \right]} \right]. \tag{19}$$

In eq. (19) we have:

$$\begin{aligned} q_p^{(i)} &= p\text{-th element of the reconstructed photon statistics at the } i\text{-th iteration}; \\ g_\mu \left[\left\{ q_p^{(i)} \right\} \right] &= \text{evaluated non-click probability from the reconstructed } q_p^{(i)}; \\ h_\mu &= \left\{ \begin{array}{ll} f_{00}^{\eta_\mu} = \frac{n_{00\eta_\mu}}{n_\mu} & \mu = 1, .., K \\ f_{01}^{\eta_\mu} = \frac{n_{01\eta_\mu}}{n_\mu} & \mu = K+1, .., 2K \\ f_{10}^{\eta_\mu} = \frac{n_{10\eta_\mu}}{n_\mu} & \mu = 2K+1, .., 3K \end{array} \right\}; \end{aligned} \tag{20}$$

being $n_{01\eta_\mu}, n_{10\eta_\mu}, n_{00\eta_\mu}$ the number single and double non-click events observed on the whole amount n_μ of experimental runs made with $\eta = \eta_\mu$.

To evaluate the confidence interval on the determination of the element $q_n^{(i)}$ we still use eq. (8), but now the Fisher information F_p on the reconstructed element is rewritten as:

$$F_p = \sum_{\mu=1}^{3K} \frac{1}{d_\mu} \left(\left. \frac{\partial d_\mu}{\partial q_p} \right|_{q_p = q_p^{(i)}} \right)^2 \tag{21}$$

with:

$$d_\mu = \frac{\sum_{p=1}^{(N+1)^2} B_{\mu p} q_p}{\sum_{\mu=1}^{3K} \left(\sum_{p=1}^{(N+1)^2} B_{\mu p} q_p \right)}.$$

The analogous of the total error $\epsilon^{(i)}$ written in eq. (10) is given by:

$$\epsilon^{(i)} = (3K)^{-1} \sum_{\mu=1}^{3K} \left| h_\mu - g_\mu \left[\left\{ q_p^{(i)} \right\} \right] \right| \tag{22}$$

which measures the distance of the reconstructed non-click probabilities from the measured ones: the algorithm is stopped when $\epsilon^{(i)}$ reaches its minimum, or goes below a certain threshold value.

Finally, the fidelity equation (11) for the reconstructed joint photon number distribution takes the form:

$$G^{(i)} = \sum_{p=1}^{(N+1)^2} \sqrt{q_p^{(theo)} \cdot q_p^{(i)}} \tag{23}$$

giving us the chance to compare the obtained $q_p^{(i)}$ with the expected ones ($q_p^{(theo)}$). In the end, here we have presented our new photon statistics reconstruction method (based on on/off detection) for a generic bipartite optical field: the next section will be dedicated to the experimental tests we made in order to check its reliability.

4. Extension to the bipartite case: experimental tests

Let us now report the experimental results obtained by applying the reconstruction method presented above to two different situations, the single photon state passing through a beam splitter (BS) and the split PDC single branch: as we will see soon, our algorithm managed to obtain a good reconstruction of the joint photon distribution in both the cases[26,27].

A. Setup A: Type-II PDC single photon source

In our first experimental setup (fig. 2)[26], a 0.2 W, 398 nm pulsed (with 200 fs pulses and 70 MHz repetition rate) laser pump was generated by second harmonic of a Ti:Sapphire laser at 796 nm; it was then injected into a $5 \times 5 \times 1$ mm type-II BBO crystal, generating entangled photon pairs by Parametric Down-Conversion. The detection of a photon on one of two correlated branches of degenerate PDC emission was then used as trigger to herald the presence of the correlated photon in the other direction.

Thus, the idler photon was addressed to an optical filter (a narrow band interference filter or a red glass, as will be specified later), collected by a lens and then sent to a silicon APD (APD1). Instead, the corresponding signal was properly filtered (with the same filter as the idler photon) and then injected into a beam splitter (BS), separating in two the optical path of the photon and thus generating a bipartite state that is the superposition of a single photon ($|1\rangle$) with the vacuum state ($|0\rangle$):

$$|\psi_{BS}\rangle = \sqrt{\tau}|01\rangle + \sqrt{1-\tau}|10\rangle \tag{24}$$

where τ is the BS transmittance.

The BS was followed on both output arms by a collection/detection apparatus, respectively called APD2 and APD3, of the same type as APD1 (all the detectors were Perkin Elmer SPCM-AQR-15 silicon APDs).

The proper set of quantum efficiencies was obtained by inserting before the BS several neutral filters (NF) of different transmittance, calibrated by measuring the

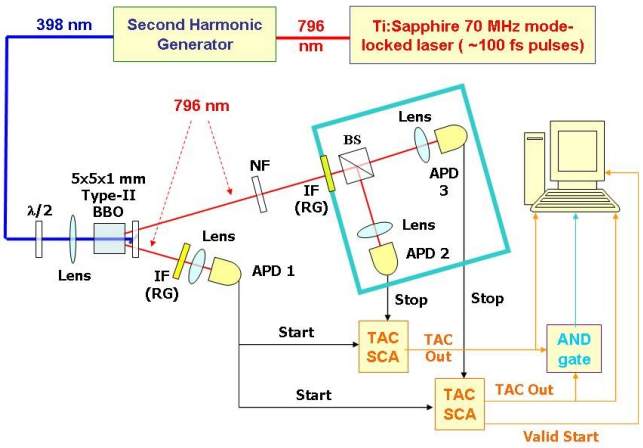

Fig. 2. schematics of the experimental setup featuring the Type-II PDC heralded photon source. The idler photon is addressed to an IF (RG) filter, collected and sent to APD1, opening a coincidence window in the TAC modules; the signal goes through the NF and the IF (RG) filters, and then is split by the BS, whose outputs are collected and sent to APD2 and APD3 to close the coincidence windows opened. The output of the two TACs is also sent to an AND logical gate whose outputs gives the number of double coincidences.

ratio between the counting rates on D2 and D3 with the filter inserted and without it.

In correspondence of the detection of a photon in arm 1, a coincidence window was opened on both detectors on arm 2: this was obtained by sending the output of D1 as Start to two Time-to-Amplitude Converters (TAC) that received the detector signal of D2 and D3 as Stop. The 20 ns coincidence window was set such to avoid spurious coincidences with PDC photons belonging to the following pulse (we remind that the repetition rate of the laser was 70 MHz).

The TAC Out outputs were then addressed both to the computer and to an AND logical gate in order to reveal coincidences between them; its output was also collected via computer, together with one TAC's Valid Start (giving us the total number of coincidence windows opened).

These four data sets allowed us to evaluate the click/non-click frequencies f_{00}, f_{01}, f_{10}, f_{11}, needed for the reconstruction of the photon statistics of the bipartite state with our recursive method (except for f_{11}). The background is estimated and subtracted by measuring the TACs and AND outputs out of the window triggered by APD1 detection; then, the maximum quantum efficiency η_{max} was calculated as the ratio between the sum of coincidences in APD2 and APD3 and the counting rate on APD1 without the insertion of any NF[31,32].

With the purpose to verify the method in different cases we considered four alternatives given by the combination of a balanced (50% - 50%) or unbalanced (40% - 60%) BS with two optical filters sets, either large band red glass filters (RG) with cut-off wave length at 750 nm, or interference filters (IF) with peak wave length at 796 nm and a 10 nm FWHM.

The first test was made with the 50%-50% BS and the interference filters: we collected data for $K = 33$ different quantum efficiencies. Elaborating these data with our reconstruction algorithm within a 3×3 Hilbert space choice ($N = 2$) lead to the reconstructed joint photon distribution shown in fig. 3: here we can appreciate how the only relevant entries are ϱ_{01} and ϱ_{10} (single photon transmitted or reflected by the beam splitter), well reproducing the inserted BS ratio.

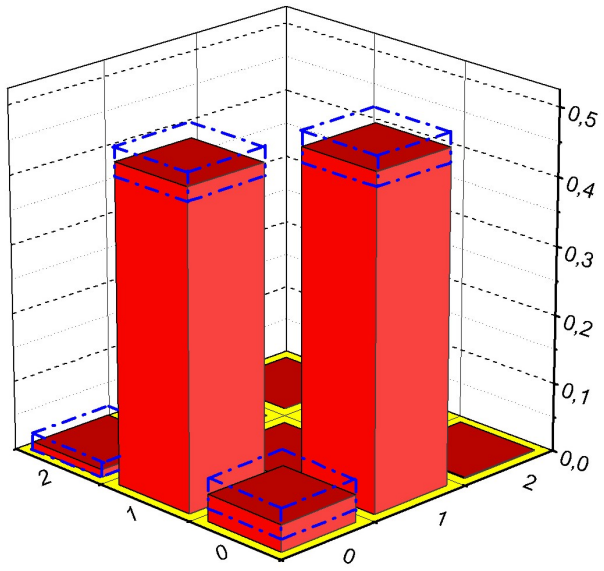

Fig. 3. reconstructed ϱ_{nk} entries of the joint photon distribution of our $|\psi_{BS}\rangle$ for the setup with 50%-50% BS and 10 nm FWHM IF: within the uncertainty intervals we can see $\varrho_{01} = \varrho_{10}$, in agreement with the BS τ value.

There is also a low but non-null vacuum component ϱ_{00}: this can be due to a non perfect background evaluation and subtraction in the experimental data, or to some light absorption in the system (maybe caused by the BS cube).

The second test was performed with the same BS but with different optical filters, namely red glass (RG) filters with $\lambda_{cut-off} = 750$ nm: the maximum quantum efficiency obtained this time was $\eta_{max} = 8,8\%$, and the acquisition was again repeated $K = 33$ times. Similar results were obtained with red glass filters.

Then we replaced the 50%-50% BS cube with an unbalanced 60%-40% BS plate, maintaining the RG large band filters: with this setup we had $\eta_{max} = 12,3\%$, and performed a $K = 41$ steps data collection. The difference between the transmitted and reflected branch of the BS was evident and in agreement with the known beam splitter ratio, also we did not have any non-null ϱ_{nk} component except for ϱ_{10} and ϱ_{01}, thus the reconstructed state

is definitely the one of eq. (24) with $\tau = 0, 4$. Finally, for the last test we replaced the RG filters with the previous IF ones obtaining a similar result.

B. Setup B: Type-I PDC thermal source

As a second example we considered a single branch of PDC emission without triggering, corresponding to a multi-thermal statistics[7].

In a setup similar to the previous one,[26], we generated PDC light by means of a $5 \times 5 \times 5$ mm Type-I BBO crystal pumped by a Q-switched (triplicated to 355 nm) Nd:Yag laser with 5 ns pulses, power up to 200 mJ per pulse and 10 Hz repetition rate. Because of the very high power of the pump beam, a state with a large number of photon was generated each pulse. We have therefore attenuated (by using 1 nm FWHM IF and neutral filters) the multithermal state before detection.

Again, the different quantum efficiencies were obtained by inserting (before the BS) Schott neutral filters, whose calibration this time was obtained by measuring the power of a diode laser before and after them, with the calibration laser injected in the same point as the PDC in order to minimize the effect due to eventual non homogeneous NF filters. The coincidence scheme was realized sending two Q-switch triggered pulses to two TAC modules as Start inputs, and the APDs outputs as Stop; then, having set properly the 20 ns coincidence window, we addressed the two TAC Out outputs to the AND logic port, and the Valid Stops to the counting modules (together with one TAC's Valid Start and the AND output). The background was estimated and subtracted in the same way as in the previous experiment.

The maximum quantum efficiency η_{max} was in this second case evaluated by multiplying the APDs nominal quantum efficiencies, the IF peak transmittance and the fiber couplers effective efficiency, measured with the diode laser: it turned out to be $\eta_{max} = 25,0\%$.

The expected on/off joint statistics for this optical state is:

$$\begin{cases} p_{00}^{\eta} = [M(M+\eta N_{ave})^{-1}]^M \\ p_{01}^{\eta} = [M(M+\eta\tau N_{ave})^{-1}]^M - p_{00}^{\eta} \\ p_{10}^{\eta} = \{M[M+\eta(1-\tau)N_{ave}]^{-1}\}^M - p_{00}^{\eta} \end{cases} \tag{25}$$

where N_{ave} is the average number of photons, M the number of propagation modes and τ the BS transmittance.

The reconstructed joint photon statistics (now upon a 17×17 truncated Hilbert space) was compared with the multithermal distribution:

$$\varrho_{nm} = \frac{(n+m+M-1)!}{n!m!(M-1)!} \cdot \frac{\left(1+\frac{N_{ave}}{M}\right)^{-M}}{\left(1+\frac{M}{N_{ave}}\right)^{m+n}} \tag{26}$$

The calculated fidelity, with the formula (11), for $i \geq 2000$ was always greater than 99%.

In summary, we can say that this experiment gave another confirm of the reliability of our algorithm, even when dealing with a larger Hilbert space.

5. Reconstruction of the non-diagonal elements

The previously described method can deliver complete information on a quantum optic state when the density matrix of such a state is diagonal, and all the non-diagonal elements are equal to zero. Obviously, a more general procedure is required which takes into account also the states in which not all the non diagonal elements vanish. In order to reconstruct also the non-diagonal elements, and thus the entire density operator, it will be shown that additional phase information is needed. Before entering into the details of our implementation, in order to introduce the theoretical method[33], let us just suppose for the moment that the state to be reconstructed is mixed with a local oscillator mode by an unbalanced beam-splitter (with high transmittance and low reflectance). It is easy to verify that, in this case, the transmitted mode is equivalent to the signal mode shifted by a displacement operator $D(\alpha) = \exp(\alpha a^{\dagger} - \alpha^* a)$, where a ($a^{\dagger}$) is the photon destruction (creation) operator associated to the signal mode and $\alpha = |\alpha| e^{i\varphi}$ is the local oscillator field amplitude. Measuring the photon statistics of the output state is equivalent to measuring the displaced Fock-state probability distribution of the signal:

$$p_n(\alpha) = \langle n, \alpha | \hat{\rho} | n, \alpha \rangle \tag{27}$$

where $|n, \alpha\rangle \equiv D(\alpha)|n\rangle$ are the displaced Fock states and $\hat{\rho}$ is the signal mode density operator. Note that p_n is now a function of the displacement α also.

For any physical state the density matrix elements $\langle k|\hat{\rho}|m\rangle$ decrease with increasing k and m, therefore $p_n(\alpha)$ can be approximated to any desired degree of accuracy by setting those elements to zero for $k, m > n_0$, where n_0 is a conveniently large integer number.

It follows that we can expand eq. 27 in the form:

$$p_n(\alpha) = \sum_{k,m=0}^{n_0} \langle n, \alpha | k \rangle \langle k | \hat{\rho} | m \rangle \langle m | n, \alpha \rangle \tag{28}$$

Expressing the displaced Fock states $|n, \alpha\rangle$ in the ordinary Fock basis, one obtains[33]:

$$p_n(\alpha) = e^{-|\alpha|^2} n! \sum_{k,m=0}^{n_0} \sqrt{k!m!} \langle k|\hat{\rho}|m\rangle \times \\ \times \sum_{j=0}^{\bar{j}} \sum_{l=0}^{\bar{l}} \frac{(-1)^{j+l} |\alpha|^{m+k+2(n-j-l)} e^{i(m-k)\varphi}}{j!(n-j)!(k-j)!l!(n-l)!(m-l)!} \tag{29}$$

where $\bar{j} \equiv min\{n, k\}$ and $\bar{l} \equiv min\{n, m\}$, so that for any value of $|\alpha|$, $p_n(\alpha)$ can be regarded as a function of φ and expanded in a Fourier series, the general component

being:

$$p_n^{(s)}(|\alpha|) = \frac{1}{2\pi}\int_0^{2\pi} p_n(\alpha)e^{is\varphi}d\varphi = \sum_{m=0}^{n_0-s} G_{n,m}^{(s)}(|\alpha|)\langle m+s|\hat{\rho}|m\rangle \quad (30)$$

with:

$$G_{n,m}^{(s)}(|\alpha|) = e^{-|\alpha|^2} n!\sqrt{m!(m+s)!}\times \times \sum_{j=0}^{\tilde{j}}\sum_{l=0}^{\bar{l}} \frac{(-1)^{j+l}\,|\alpha|^{2(m+n-j-l)+s}}{j!(n-j)!(m+s-j)!l!(n-l)!(m-l)!} \quad (31)$$

where $\tilde{j} \equiv min\{n, m+s\}$. We notice that $p_n^{(s)}(|\alpha|)$ is related to the density matrix element whose row and column indices differ by s. If the photon number distribution $p_n(\alpha)$ is measured for $n = 0, 1, \ldots, N$, with $N \geq n_0$,eq. (30) for each s represents a system of $(N+1)$ linear equations linking $(N+1)$ measured quantities $p_n^{(s)}$ to (n_0+1-s) parameters (the unknown density matrix elements). This system is clearly overdetermined, so it can be inverted using the least squares method in order to obtain the density matrix elements from the measured probabilities.

The reconstructed off-diagonal density matrix elements can thus be obtained as:

$$\langle m+s|\hat{\rho}_{rec}|m\rangle = \sum_{n=0}^{N} F_{n,m}^{(s)}(|\alpha|)p_n^{(s)}(|\alpha|) \quad (32)$$

with:

$$F_{n,m}^{(s)}(|\alpha|) = \{[G_{n,m}^{(s)}(|\alpha|)]^T G_{n,m}^{(s)}(|\alpha|)\}^{-1}[G_{n,m}^{(s)}(|\alpha|)]^T \quad (33)$$

The F matrix satisfies the condition:

$$\sum_{n=0}^{N} F_{m',n}^{(s)}(|\alpha|)G_{n,m}^{(s)}(|\alpha|) = \delta_{m,m'} \quad (34)$$

for $m, m' = 0, 1, \ldots, n_0 - s$, so that from the exact probabilities the correct density matrix elements are found ($\hat{\rho}_{rec} \equiv \hat{\rho}$). Furthermore, the least squares method ensures that the ${}^*p_n^{(s)}$ calculated from $\hat{\rho}_{rec}$ according to eq. (30) best fits the measured quantities such that:

$$\sum_{m=0}^{N} ({}^*p_n^{(s)} - p_n^{(s)})^2 \quad (35)$$

is minimized.

In conclusion, combining eq.s (32) and (30), we find out the formula for the direct sampling of the density matrix from the measured photon number distribution of the displaced state[33]:

$$\langle m+s|\hat{\rho}_{rec}|m\rangle = \frac{1}{2\pi}\sum_{n=0}^{N}\int F_{n,m}^{(s)}(|\alpha|)e^{is\varphi}p_n(\alpha)d\varphi \quad (36)$$

It is worth mentioning that this method, given that the $p_n(\alpha)$ are known, requires only the value of φ to be varied.

Let us now extend our method for the case of non-perfect detection, in which the detection efficiency η is less than unity. The effective measured photocount distribution $P_k(\alpha)$ is related to the photon number distribution $p_n(\alpha)$ as follows:

$$P_k(\alpha) = \sum_{n=0}^{\infty} M_{k,n}(\eta)p_n(\alpha) \quad (37)$$

where $M_{k,n}(\eta)$ is:

$$M_{k,n}(\eta) = \begin{cases} \binom{n}{k}\eta^k(1-\eta)^{n-k} & k \leq n \\ 0 & k > n \end{cases} \quad (38)$$

since $\eta^k(1-\eta)^{n-k}$ is the probability to detect k among n incoming photons and $\binom{n}{k}$ is the number of possible k-photons subsets. So, the equivalent of eq.(30) for the measured quantities $P_n^{(s)}(|\alpha|)$ yields:

$$P_n^{(s)}(|\alpha|) = \sum_{m=0}^{n_0-s} G_{n,m}^{(s)}(|\alpha|\,,\eta)\langle m+s|\hat{\rho}|m\rangle, \quad (39)$$

where the new matrices:

$$G_{n,m}^{(s)}(|\alpha|\,,\eta) = \sum_{k=0}^{\infty} M_{n,k}(\eta)G_{k,m}^{(s)}(|\alpha|), \quad (40)$$

obtained from the $G_{k,m}^{(s)}(|\alpha|)$ defined in eq. (31), can be inverted in the same manner described above to obtain some matrices $F_{m,n}^{(s)}(|\alpha|\,,\eta)$ to be used, as in eq. (36), to reconstruct the density matrix.

6. Experiment: full density matrix reconstruction for a coherent state

The key element for the reconstruction of non-diagonal elements in the density matrix of the measured state is a sort of asymmetric homodyne detection in which the signal mode and a local oscillator are mixed by an unbalanced beam splitter. In our scheme, actually, the local oscillator is not an external source but it is obtained by the same source as the signal divided in two by a 50/50 beam splitter.

To be more precise, the source beam enters in a Mach-Zehnder interferometer in which the part reflected by the first beam splitter is taken as the signal, as it travels along the "long" path inside the interferometer, while the transmitted portion is regarded as the local oscillator. The two modes are then mixed by the second beam splitter, which is effectively used to perform a sort of unbalanced homodyning. It is possible to change the length of the optical path in the long arm of the inteferometer, thus varying the phase or the signal mode with respect to the reference mode.

The expression of the mean number of photons at the output port of the interferometer it is easy to be calculated and yields:

$$\langle \hat{n}_o \rangle = Tr[\hat{a}_o^\dagger \hat{a}_o \hat{\rho}] = \langle \hat{n}_i \rangle \frac{1 - cos(\varphi)}{2}, \qquad (41)$$

where $\hat{\rho}$ and $\hat{n}_i$ are, respectively, the density and the photon number operators for the input state. We remind here that the non-click probability p_0, which is the quantity to be actually measured, for a coherent state of amplitude ν, reads:

$$p_0(\eta) = \sum_{n=0}^{\infty} (1-\eta)^n p_n = \sum_{n=0}^{\infty} (1-\eta)^n \frac{|\nu|^{2n} e^{-\eta|\nu|^2}}{n!} \qquad (42)$$

which obviously is a function of the overall quantum efficiency η of the detection system. In our case, p_0 is also a function of φ since $|\nu|^2$ can be derived from eq.41 ($|\nu|^2 = \langle \hat{n} \rangle$).

The theoretical method exposed in the previous section leads to the possibility of a direct experimental sampling of the density operator of the initial state by performing photon distribution reconstructions[21,22] of the state exiting the interferometer for a suitable number of φ values.

We point out that our scheme allows to estimate the error in real time, that it is suitable both for pure and mixed states and that statistic information is obtained by sampling a discrete matrix rather than measuring a continuous distribution in phase space as homodyne quantum tomography schemes.

A. Setup

In our set-up (see fig.4)the signal state is the output of a He-Ne laser ($\lambda = 632.8$ nm), which is lowered to single photon regime by neutral filters. The spatial profile of the signal is purified from non-gaussian components by a spatial filter realized by two converging lenses and a $100\mu m$ diameter wide pinhole. An iris just after the pinhole ensures the selection of a single Gaussian spatial mode. The laser cavity is also preserved by backreflections, which may cause instability, by means of an optical isolator consisting in a Faraday rotator between two polarizers. The second polarizer (let us name it B) angle is shifted of 45 degrees with respect to the first (A), so that the light transmitted by the latter, whose polarization is rotated by 45 degrees by the Faraday rotator, is all transmitted also by the second. Since the polarization rotation by Faraday effect is in the same direction regardless of the laser propagation direction, any backreflected light passing through B, would suffer another 45 degrees rotation before reaching a polarizer and would thus be stopped, being orthogonal to the polarizer angle.

After a beam-splitter, part of the beam is addressed to a control detector in order to monitor the laser amplitude fluctuations, while the remaining part is sent to the interferometer, its main structure consisting in a single invar block custom designed and developed at INRIM.

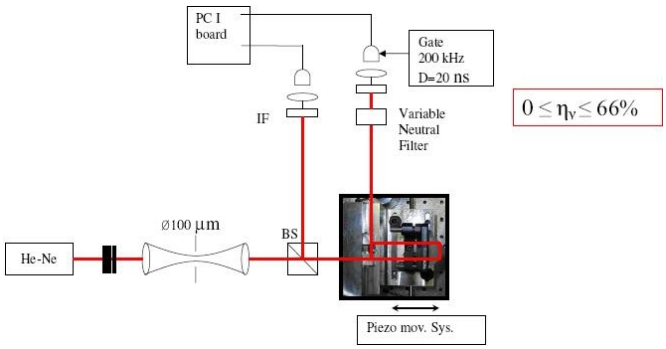

Fig. 4. *Setup for the reconstruction of the density matrix for a coherent state. The emission of a He-Ne laser ($\lambda = 632.8$ nm) is lowered to single photon regime by neutral filters. A spatial filter realized by two converging lenses and a $100\mu m$ diameter-wide pinhole purifies the shape of the signal and allows to select a single spatial mode. A beam-splitter reflects part of the beam to a control detector used to monitor the laser amplitude fluctuations, while the remaining part is sent to the interferometer. The phase between the "short" and "long" paths in the interferometer can be changed by driving the position of the reflecting prism by means of a PI piezo-movement system. A set of variable neutral filters allows to collect photons for different values of the quantum efficiency. The detectors used are Perkin-Elmer Single Photon Avalanche Photodiode(SPCM-AQR) gated by a 20 ns wide time window with (repetition rate = 200 kHz). A single run consists of 5 repetitions of 4 seconds acquisitions and events are recorded by a NI-6602 PCI counting module.*

A PI piezo-movement system allows to change the phase between the "short" and "long" paths by driving the position of the reflecting prism with nanometric resolution and high stability.

For each position of the prism, the "no-click" probabilities are collected for different sets of neutral filters, and thus, for different quantum efficiencies.

The detector, a Perkin-Elmer Single Photon Avalanche Photodiode (SPCM-AQR), is gated by a 20 ns wide time window with a repetition rate of 200 kHz. In order to obtain a reasonable statistics, a single run consists of 5 repetitions of 4 second acquisitions. Events are recorded by a NI-6602 PCI counting module. In this case, since all the attenuations in front of the detectors can be included in the generation of the state, the overall maximum quantum efficiency is assumed to be 66.5%, as the nominal efficiency declared by the manufacturer data-sheet of the photodetectors.

B. Experimental results

In our preliminary experiment[34] we consider $\mathcal{N}_\varphi = 11$ number of different phases and reconstruct the corre-

sponding photon distributions using the method exposed in the previous sections. Due to the small number of phases considered, only the diagonal and the first off-diagonal elements of the density matrix can be reconstructed. The results are shown in Fig. 5 where we plot the reconstructed ($\rho^{rec}_{n,m}$), the expected ($\rho^{exp}_{n,m}$) density matrix elements and the absolute difference $\delta = \left|\rho^{rec}_{n,m} - \rho^{exp}_{n,m}\right|$. The reconstructed ρ^{rec} corresponds to a coherent state $|\alpha\rangle$ with energy $|\alpha|^2 = 3.06$. Considering the small amount of data, the agreement between ρ^{rec} and ρ^{exp} is good. Another measurement has been performed with the same setting but without unbalancement in the second beam splitter, and the collected data $p_0(\eta)$ for several values of φ are being evaluated right now.

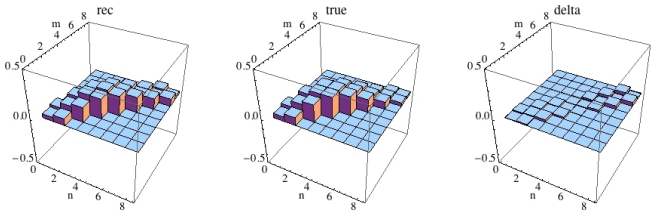

Fig. 5. *In order, from left to right, the three plots show the reconstructed density matrix (rec), $\rho^{rec}_{n,m}$, for the coherent state, the expected matrix (true), $\rho^{exp}_{n,m}$, and the absolute difference $\delta = \left|\rho^{rec}_{n,m} - \rho^{exp}_{n,m}\right|$ (delta) between the two. In particular, the last plot show good agreement between the reconstruction results and the theoretical values in view of the small number of phases considered for reconstruction.*

7. Acknowledgements

This work has been supported by EU project Qu-Candela, by Compagnia di San Paolo, by PRIN 2007FYETBY (CCQOTS), PRIN 2005023443-002, by Regione Piemonte (E14) and partially supported by the CNR-CNISM convention.

References

1. The Physics Of Quantum Information, Ed. by D. Bouwmeester, A. Ekert, A. Zeilinger (Springer, 2000);
2. M. Genovese, Phys. Rep. 413/6 (2005);
3. W. Vogel, D.G. Welsch, Quantum Optics - An Introduction (Wiley-VCH, Berlin, 2001);
4. W.P. Schleich, Quantum Optics In Phase Space (Wiley-VCH, Berlin, 2001);
5. J. Perina, Z. Hradil, B. Jurco, Quantum Optics and Fundamental Physics (Kluwer, Dordrecht, 1994);
6. U. Leonhardt, Measuring The Quantum State Of Light (Cambridge Univ. Press, Cambridge, 1997);
7. L. Mandel, E. Wolf, Optical Coherence And Quantum Optics (Cambridge Univ. Press, Cambridge, 1995);
8. D.T. Smithey, M. Beck, M.G. Raymer, and A. Faridani, Phys. Rev. Lett. 70, 1244 (1993);
9. G. M. D'Ariano, C. Macchiavello, and M.G.A. Paris, Phys. Rev. A 50, 4298 (1994);
10. M. Raymer, M. Beck in Quantum States Estimation, M. G .A Paris and J. Řeháček Eds., Lect. Not. Phys. 649 (Springer, Berlin-Heidelberg, 2004);
11. G.M. D'Ariano et al., in Quantum States Estimation, M.G.A Paris and J. Řeháček Eds., Lect. Not. Phys. 649, (Springer, Berlin-Heidelberg, 2004);
12. G.M. D'Ariano and L. Maccone, Electronic Notes in Discrete Mathematics 20, 133 (2005);
13. G. Zambra, M. Bondani, A.S. Spinelli, A. Andreoni, Rev. Sci. Instrum. 75, 2762 (2004);
14. E. Hergert, Single Photon Detector Workshop (Gaithersburg, NIST, 2003);
15. J. Kim, S. Takeuchi, Y. Yamamoto, H.H. Hogue, Appl. Phys. Lett. 74, 902 (1999);
16. G. Di Giuseppe, A.V. Sergienko, B.E.A. Saleh, M.C. Teich, in Quantum Information and Computation, Proceedings of the SPIE 5105, 39 (2003);
17. M. Munroe, D. Boggavarapu, M.E. Anderson, M.G. Raymer, Phys. Rev. A 52, R924 (1995);
18. F. Zappa, A.L. Lacaita, S.D. Cova, P. Lovati, Opt. Eng. 35, 938 (1996);
19. D. Mogilevtsev, Opt. Comm. 156, 307 (1998);
20. D. Mogilevtsev, Acta Phys. Slov. 49, 743 (1999);
21. A.R. Rossi, S. Olivares, M.G.A. Paris, Phys. Rev. A 70, 055801 (2004);
22. A.R. Rossi, M.G.A. Paris, Eur. Phys. J. D 32, 223 (2005);
23. G. Zambra et al., Phys. Rev. Lett. 95, 063602 (2005);
24. G. Brida et al., Laser Physics 16, 385 (2006);
25. G. Brida et al., Open Syst. & Inf. Dyn. 13, 333 (2006);
26. G. Brida, M. Genovese, M.G.A. Paris, F. Piacentini, Opt. Lett. 31, Issue 23 (2006);
27. G. Brida et al., Opt. & Spectr. 103, 95 (2007);
28. A.P. Dempster et al., J. R. Statist. Soc. B 39, 1 (1977);
29. G. Brida et al., Journ. Mod. Opt. Special Issue: Single Photon, in press;
30. G. Brida et al., Int. J. Quant. Inf. 5, Nos. 1-2, 265 (2007);
31. G. Brida et al., , J. Mod. Opt. 47, 2099 (2000);
32. G. Brida et al., Las. Phys. Lett. 3, 115 (2006);
33. T. Opatrný, D.G. Welsh, Phys. Rev. A 55, 1462 (1997), *55*, 1462.
34. G. Brida et al., Int. J. Quant. Inf., in press.